AMERICAN JOURNAL OF PHARMTECH RESEARCH

Journal home page: http://www.ajptr.com/

Synthesis, DNA Binding, Photo Nuclease and Antibacterial PDT of Iron Complexes of Phenanthroline Based Photosensitizers

Chittanahalli N. Sudhamani[1], Halehatty S. Bhojya Naik[1]*, Kalligundi R. Sangeetha Gowda[1] and M. Giridhar[1]

1.Department of Studies and Research in Industrial Chemistry, School of Chemical Sciences, Kuvempu University, Shankaraghatta-577 451, INDIA

ABSTRACT

Fe(II) complexes $[Fe(mqs)(B)_2](PF_6)$**(1)-(3)** of 2-thiol 4-methylquinoline and phenanthroline bases (B), viz 1,10-Phenanthroline (phen in **1**), Dipyrido[3,2-*d*:2',3'-*f*]quinoxaline (dpq in **2**) and Dipyrido[3,2-*a*:2′,3′-*c*]phenazine (dppz in **3**) have been prepared and characterized. The DNA-binding behaviors of these three complexes were investigated by absorption spectra, viscosity measurements and thermal denaturation studies. The DNA-binding constants for complexes 1, 2 and 3 were determined to 2.4 $x10^4$, 1.3 x 10^5 and 4.2 $x10^5$ M^{-1}, respectively. The experimental results suggest that these complexes interact with DNA through groove binding mode. The photo induced cleavage studies shows that the complexes possess photonuclease property against pUC19 DNA under UV–Visible irradiation *via* a mechanistic pathway involving formation of singlet oxygen as the reactive species. Antibacterial PDT for E. coli strain, the control group showed a significantly higher ($p<0.05$) bacterial growth (1.5 x 10^8 CFU/mL), while the complex (3) group presented no significant reduction ($p>0.05$) in the CFU counts. The complex (3)/Light group presented a significant decrease in the CFU counts ($p<0.05$) compared with the control group (71.64% for E. coli).

Keywords: groove binding; metal complexes; singlet oxygen; photonuclease activity; antibacterial PDT.

*Corresponding Author Email: hsb_naik@rediffmail.com

Received 18 January 2014, Accepted 24 January 2014

Please cite this article in press as: Naik B *et al.*, Synthesis, DNA Binding, Photo Nuclease and Antibacterial PDT of Iron Complexes of Phenanthroline Based Photosensitizers. American Journal of PharmTech Research 2014.

INTRODUCTION

The interaction of metal complexes with DNA is a center of research interest in bioinorganic chemistry. The development of artificial nucleases is an important aspect in the areas of biotechnology, drug design and molecular biology[1–4]. For this purposes tranisition metal complexes have been employed, becuase of their versatile electronic and structural features, but also due to the fact that the DNA binding and cleavage ability of metal complexes can be tuned by changing the coordination environment[5, 6]. There is already a considerable literature involving the practical use of transition metal complexes as chemical nucleases. However, most of these complexes contain only transitional metal complexes of 1, 10-phenanthroline and their modified variants are widely employed for studies of DNA in view of their utility in several research areas, including bioinorganic and biomedicinal chemistries[7–10].

Further, selenium-containing heterocyclic compounds shows have remarkable reactivities and chemical properties, as well as pharmaceutical applications. Despite the high toxicity of many selenium compounds, organic derivatives of selenium have been synthesized as anticancer agents and for other medicinal applications. They also play key role in decreasing oxidative stress in HIV-infected cells and possibly suppressing the rate of HIV replication. The development of organoselenium compounds with higher anticarcinogenic efficacy but better tolerance continues to be a priority in chemotherapy research. From a chemical point of view, selenium (Se) resembles sulfur (S) in many of its properties, thus, Se and S may be considered to be isosteric[11-13].

Earlier reports on iron complexes are mainly intended to model the structural and functional properties of glycopeptide antitumor, antibiotics and bleomycins (BLMs)[14, 15]. Iron complexes extensively been used to cleave DNA and such complexes are used for DNA foot printing purposes[15–17]. Iron polypyridyl complexes, which known may cleave DNA by generating Reactive Oxygen Species in vitro, could be potential anticancer drugs by killing cancer cells[18–20]. Photodynamic therapy (PDT) has historically been used as a means to treat cancerous tumors but has recently been used to kill bacterial cells through the use of targeted photosensitizers. This therapy is defined as an oxygen-dependent photochemical reaction that occurs upon light mediated activation of a photosensitizing compound leading to the generation of cytotoxic reactive oxygen species, predominantly singlet oxygen[21]. This photodynamic approach could be a useful alternative to systemic medications in treating localized infections, thus avoiding the development of microbial resistance to systemic drugs. Photodynamic antimicrobial

chemotherapy signifies an alternate antibacterial, antifungal, and antiviral treatment against drug resistant organisms[22].

This work presents a new approach to designing iron-based photonucleases and explore the photosensitizing effect of Iron complexes containing se and N,N donor heterocyclic bases by investigate the effect on antibacterial PDT.

MATERIALS AND METHOD

All reagents and solvents required in this study were of AR grade, purchased from Himedia (India). The solvents were purified and used. The $FeSO_4 7H_2O$, 1,10-Phenanthroline and *Tris*-HCl were purchased from Merck (India), calf thymus (ds)DNA and supercoiled (SC) pUC19 DNA were purchased from Bangalore Genie (India) and Agarose (molecular biology grade) ethidium bromide were purchased from Himedia (India). *Tris*-HCl buffer solution used for binding was prepared using deionized double-distilled water.

Elemental analyses were done on Perkin-Elmer (Waltham, MA, USA) Model 240-C CHN analyzer. The molar conductivities of the complexes in dimethyl formamide (DMF) solution (10^{-3} M) at room temperature were measured using an Equip- Tronic (India) Digital conductivity meter model No. EQ-660A. Magnetic susceptibilities of the solid complexes were measured employing Gouy balance at room temperature (28 ± 2 ^{o}C). The electronic spectra of the complexes were measured using Shimadzu spectrometer model UV-1650 PC double beam spectrophotometer. Viscosity measurements were carried out at 25± ^{o}C) using semi microdilution capillary viscometer at room temperature. Infrared (IR) spectra were recorded in 4000–250 cm^{-1} region using KBr pellets on Shimadzu (Kyoto, Japan) FTIR-8400S. The DNA binding experiments were carried out in *Tris*-HCl buffer (*Tris*-HCl buffer containing 50 mM NaCl, pH 7.2) in absorption and viscosity measurements and phosphate buffer (1 mM Phosphate, pH 7, 2 mM NaCl) was used for thermal denaturation. The calf thymus(ds) DNA in the buffer medium gave a ratio of UV absorbance at 260 and 280 nm of ca. 1.9:1, suggesting the DNA are apparently free from protein. The concentration of DNA was estimated from its absorption intensity at 260 nm with a known molar absorption coefficient value of 6600 dm^3 mol^{-1} cm^{-1} [23]. Diode laser (660 nm, 100 mW) was used as light source for antibacterial PDT.

Absorption titration experiments were performed by varying the concentration of the CT DNA with the metal complex concentration. The absorption data were analyzed for an evaluation of the intrinsic binding constant K_b using reported procedure[24]. Viscosity measurements were carried out using a semi microdilution capillary viscometer at room temperature. Each

experiment was performed three times and an average flow time was calculated. Data were presented as ($\eta|\eta_o$) *Vs* binding ratio, where η is the viscosity of DNA in the presence of complex and η_o is the viscosity of DNA alone. Thermal denaturation experiments were carried out by monitoring the absorption of CT DNA in 50 μM concentrations for the nucleotides at 260 nm with different temperatures in the presence (10 μM complex) and the absence of each complex. The melting temperature (Tm, the temperature at which 50% of double-stranded DNA becomes single stranded) and the curve width (σ_T), the temperature range between which 10% and 90% of the absorption increases occurred) were recorded.

The cleavage of DNA was monitored using agarose gel electrophoresis. Supercoiled pUC19DNA (0.5 μg) in *Tris*-HCl buffer (50 μM) with 50 μM NaCl (pH 7.2) was treated with metal complex (40 and 60 μM) followed by dilution with *Tris*- HCl buffer to a total volume of 20 μl. The samples were incubated for 1 h at 37 ^{o}C. A loading buffer containing 25% bromophenol blue, 0.25% xylene cyanol and 30% glycerol were added and electrophoresis was performed at 50 V for 3 h in TBE buffer using 0.8% agarose gel containing 1.0 μg/ml ethidium bromide. The samples were irradiated for 60 min inside the sample chamber. Bands were visualized using UV light and photographed. The cleavage efficiency was measured by determining the ability of the complex to convert the SC DNA to nicked circular form (NC) and linear form (LC).

Bacterial strains and growth conditions

Escherichia coli 25922, was grown aerobically overnight in LB broth (1% tryptone, 0.5% yeast extract, 0.5% NaCl w/v) at 37 ^{0}C.

PDT protocol

Bacterial cultures were diluted in fresh LB broth to obtain a cell density of 1.5 x 10^8 cfu/ml and, were separated into 3 groups for further studies. All groups were mixed for volume homogenization. The Control group (tube 1) contained E. coli strain, but no dye or light was applied. The Dye group (tube 2) contained E. coli strain and appropriate concentration of the complex 3 under investigation, incubated in foil-covered tubes to avoid accidental exposure to the light, which was left for 5 min, but no light was applied; The Complex 3 /Light group (tube 3) contained E. coli strain and appropriate concentration of the complex 3; illumination with the 500W halogen–tungsten lamp source at a distance of 20 cm was performed, characterizing the PDT protocol. In tube 3, the inoculum was left in contact with complex 3 for 5 min without shaking (pre-irradiation time) to allow greater absorption of dye by the bacteria.

All groups at 1.5 x 10^8 CFU/mL concentration were mixed and subjected to serial dilutions in 10 mL tubes containing LB broth until reaching dilutions of 10^{-6} CFU/mL (final concentration of

1.5x 10^2 CFU/mL). Diluted tube mixtures were seeded onto Petri dishes containing 20 mL of LB agar medium according to the Pourplate method and were incubated at 37ºC for 48 h. visual counting of CFUs was done under optical microscopy using pencil marks on dishes. Data were analyzed by one-way ANOVA and Tukey's HSD test at 5% significance level.

Synthesis and Characterization

The compound (mqs) 2-seleno 4- mehtylquinoline,[25,26] dpq ligand (dipyrido[3,2-*d*:2′,3′-*f*]quinoxaline) and dppz ligand dipyrido[3,2-*a*:2′,3′-*c*] phenazine were prepared by reported procedure [27-29]. Synthesis of iron(II) complexes containing 2-seleno 4-mehtylquinoline and as ligands are described subsequently.

Synthesis of complexes $[Fe(mqs)(B)_2](PF_6)$ (1)-(3)*:* mqs: 2-seleno 4- mehtylquinoline and B = phen, **1**; dpq, **2**, dppz ,**3**

The complexes were synthesized by following the same general procedure. Solution of ammonium ferrous sulfate (1 mmol, 0.404 g) and solution of the mqs (1 mmol, 0.222 g) was stirred for 30 min. To the above reaction mixture, 1 mmol of 10 ml methanolic solution of heterocylclic base was added and the stirring was continued for 15 min more. Thus obtained solution was treated with a methanolic solution of NH_4PF_6 to precipitate a red solid that was isolated by filtration and washed with cold methanol followed by diethyl ether and finally dried.

$[Fe(mqs)(phen)_2]PF_6$(1).

Yield 78%, C, Anal. Calc. for $C_{34}H_{24}F_6FeN_5PSe$(%): C, 52.20; H, 3.09; N, 8.95. found (%): C, 52.24; H, 3.10; N, 8.90. IR (KBr) cm^{-1}: 2492, 1621, 843, 438, 372 UV-Visible. λ_{max} (nm): 282, 335, 520. μ_{eff} = 2.81 B.M. Ω_M = 170 mhos cm^2mol^{-1}

$[Fe(mqs)(dpq)_2]PF_6$(2).

Yield 71%, Anal. Calc. for $C_{34}H_{24}F_6FeN_9PSe$ (%): C, 51.49; H, 2.73; N, 14.22. found (%): C, C, 51.47; H, 2.75; N, 14.22. IR (KBr) cm^{-1}: 2488, 1629, 845, 446, 374. UV-Visible. λ_{max} (nm): 255,292, 320, 355, 420 516. μ_{eff} = 2.77 B.M. Ω_M = 155 mhos cm^2mol^{-1}

$[Fe(mqs)(dppz)_2]PF_6$(3).

Yield 69%, Anal. Calc. for $C_{46}H_{28}F_6FeN_9PSe$(%): C, 56.00; H, 2.86; N, 12.78. found (%): C, 56.03; H, 2.88; N, 12.73. IR (KBr) cm^{-1}: 2491, 1634, 847, 448, 380. UV-Visible. λ_{max} (nm): 248, 279, 331,368, 422, 522, μ_{eff} = 2.81B.M. Ω_M = 159 mhos cm^2mol^{-1}

The complexes are soluble in dimethylformamide (DMF), dimethyl sulfoxide (DMSO) and buffer solution. The complexes are sufficiently stable in the solid and solution phases.

RESULTS AND DISCUSSION

Characterization of metal complexes

The ligand and complexes employed in this work have been characterized by elemental analysis, UV/Visible, IR and magnetic susceptibility; these are summarized in the experimental section. The formula of the complexes $[Fe(mqs)(phen)_2](PF_6)$(1), $[Fe(mqt)(dpq)_2](PF_6)$(2) and $[Fe(mqt)(dppz)_2](PF_6)$(3) respectively. These new complexes are soluble in DMF, DMSO and in buffer (pH 7.2) solution and stable in the solid as well as in a solution phase. The molar conductance values of the complexes in DMF solutions fall in the range 155–170 ohm^{-1} cm^2 mol^{-1}, demonstrating their electrolytic nature.

The UV-Visible spectra of the ligands and its complexes were recorded in DMF at 10^{-3} M concentration. The electronic spectrum for complexes 1, 2 and 3 shows a prominent broad band at 520 nm, 516 nm and 522 nm respectively ascribed to the d-d transition, which are followed by a strong bands in the UV region assigned to ligand to metal charge transfer (LMCT) transitions. The dpq and dppz complexes show a moderately strong band near 422 nm possibly due to n-π* transition involving the quinoxaline or phenazine moieties of the ligands and this band is not observed in the phen complexes.

The important IR spectral assignments of Fe(II) complexes of mqs ligand show absorption bands in the region 1621–1634 cm^{-1} and 2488–2492 cm^{-1}, which can be assigned to ν(C=N) and ν(C-SeH) vibrations, respectively. In IR spectra of the complexes, the band due to ν(C-SeH) shifted to a lower frequency to the extent of 25–38 cm^{-1} indicating the involvement of selenium atom of the ligand in bonding with metal ion through deprotonation. The band due to ν(C=N) also suffers a negative shift by 25–35 cm^{-1} suggested the involvement of nitrogen in the coordination with the Fe(II) ion. The complexes show low-frequency bands in the region 438–448 cm^{-1} and 372–380 cm^{-1}, which are assigned to ν(M-N) and ν(M-Se) bonds,respectively.,[30] In addition, the IR spectrum of the PF_6 salt of each complex showed a strong band in the region 843–847 cm^{-1}, ascribable to the counter anion[31].

DNA Binding Experiments

Electronic Absorption Titrations

The binding interaction of the Fe(II) complexes with CT-DNA was monitored by UV-Visible spectroscopy. The absorption spectra of the complexes in the absence and presence of calf thymus DNA are shown in Figure. 1(a) and 1(b). Generally, hypochromism and bathochromism with increasing CT-DNA concentration. The binding results show that the bathochromic shift of

2–3 nm along with significant hypochromicity 30% of observed in of DNA to complex solution representing appreciable groove binding propensity of the complexes to the CT DNA. In order to compare the binding strength of the complexes, their intrinsic binding constants (K_b) with CT-DNA have been determined from the decay of the absorbance. The intrinsic binding constant (K_b) values are in the range of 2.4 x10^4 – 4.2 x10^5 M^{-1} follows the order (**3**) > (**2**) > (**1**). The dpq and dppz showed significantly higher DNA binding possibly due to the presence of the quinoxaline and phenazine rings favoring partial intercalation into the DNA bases through its extended planar aromatic ring. The low value of *s* (~0.2) is indicative of more surface aggregation and/or groove binding than any intercalation to the DNA base pairs [32].

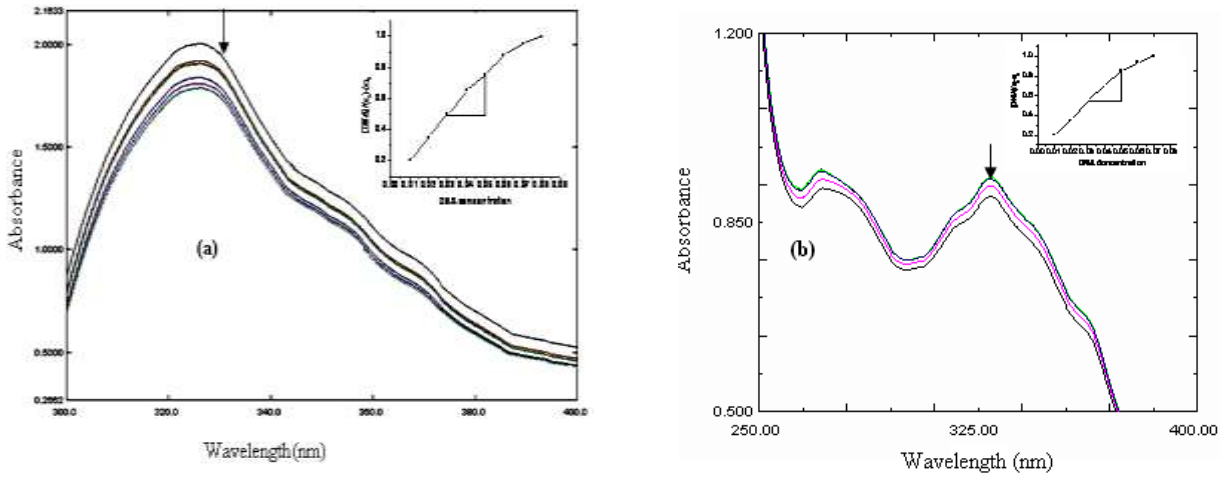

Figure 1: Absorption spectra of complexes in *Tris*-HCl buffer upon addition of DNA. [Complex] = 0.5 μM, [DNA] = (0–100 μM). Arrow shows the absorbance changing upon increase of DNA concentration. The inner plot of [DNA]/ε_a-ε_f *vs* [DNA] for the titration of DNA with complex. (a) complex (1), (b) complex (2).

Viscosity Measurements

To further clarify the binding mode between the complex and the DNA, measurements were carried out on CT-DNA by varying the concentration of the complexes. Hydrodynamic measurements, which are sensitive to length change (i.e., viscosity, sedimentation), are regarded as the least ambiguous and the most critical tests for the binding mode in solution in the absence of crystallographic structural data. A classical intercalation mode could result in the lengthening of the DNA helix as the base pairs are separated to accommodate the binding complex, leading to an increase in DNA viscosity. In contrast, complexes binding to DNA grooves result in minor variation or no variation in the viscosity of the DNA solution[33, 34].

Our data show that there is marginal increase of the relative viscosity is observed on the addition of the complexes to the DNA solution and the values of relative viscosity (η/η_0) (where η and η_0 are the specific viscosities of DNA in the presence and absence of the complexes) are plotted against [M]/[DNA] (Fig. 2), signifying the groove-binding nature of the complexes. This result further suggested groove- binding mode of the complex with DNA and also parallel to the above spectroscopic results. The values of relative viscosity (η/η_0) (where η and η_0 are the specific viscosities of DNA in the presence and absence of the complexes) are plotted against [M]/ [DNA].

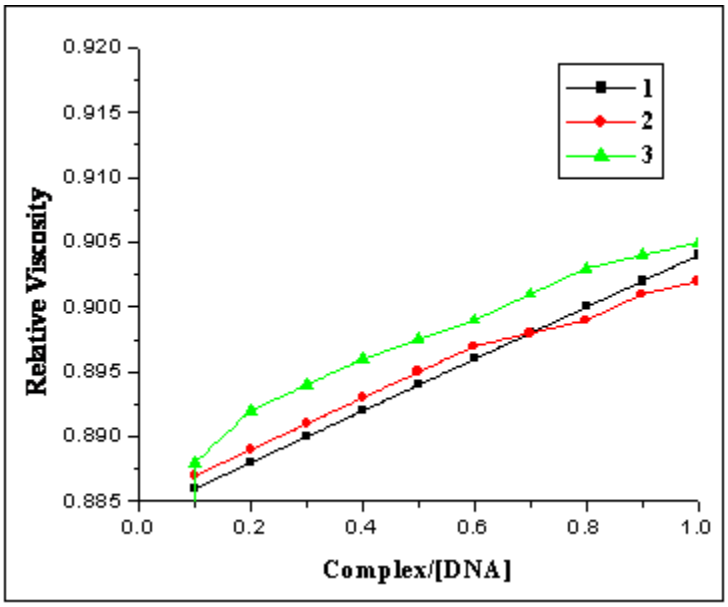

Figure 2: Plot of relative viscosity vs [Complex]/[DNA]. Effect of Fe(II) complexes on the viscosity of CT-DNA at 25 ^{0}C. Complex = 0-100 μM, [DNA] = 50 μM.

DNA Melting Experiment

The DNA melting experiments were carried out by monitoring the absorption intensity of CT-DNA at 260 nm at various temperatures both in the absence and presence of the complexes. Thermal denaturation studies of DNA are useful in establishing the extent of binding[35]. It is well known that when the temperature in the solution increases, the doublestranded DNA gradually dissociates to single strands, and generates a hypochromic effect on the absorption spectra of DNA bases(λmax = 260 nm)[36]. The melting temperature T_m, which is defined as the temperature where half of the total base pairs are unbound, is usually introduced. It is determined from the thermal denaturation curves of DNA by monitoring the changes of absorption spectra of DNA bases (λ = 260 nm).

As shown in Fig. 3, the Tm DNA was found to be 60 under experimental conditions. Under the same set of conditions, addition of Fe(II) complexes a moderate positive shift in the DNA melting temperature (Δ*T*m) ranging from 1.2 to 3.1 is observed on the addition of the Complexes **(1)-(3)** to DNA. The low value of Δ*T*m primarily suggest the groove binding nature of the complexes to DNA in preference over an intercalative mode of binding to DNA that normally gives significantly high positive Δ*T*m values[37].

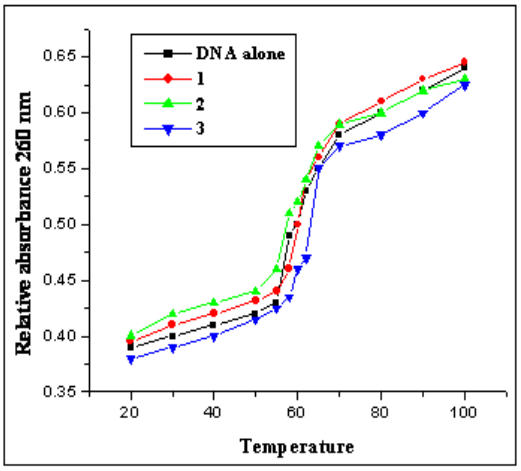

Figure 3. Thermal denaturation of CT-DNA in the absence and presence of Fe(II) complexes. [DNA]= 50 μM, [complex] = 10 □ M, Buffer: Phosphate.

Photo-induced DNA cleavage activity

The photoinduced DNA cleavage activity of the Fe(II) complexes is studied using SC pUC19 DNA (33.3 *í*M, 0.2 *íg*) in a medium of Tris-HCl/NaCl (50 mM, pH, 7.2) buffer on irradiation with UV light of 365 nm and monitored by gel electrophoresis. The extent of DNA cleavage from SC to the nicked circular (NC) form is shown in Fig. 4-6 (gel electrophoresis diagrams). The DNA binder heterocyclic bases dpq and dppz have photoactivatable quinoxaline and phenazine moieties with conjugated C=N bonds that could generate photoexcited 3(*n*-*π**) or 3(*π*-*π**) state(s) effecting DNA cleavage following an oxidative pathway. The cleavage activity at 365 nm follows the order: **3** > **2** >**1**.

The mechanistic aspects of the photo-induced DNA cleavage activity of the complexes at 360 nmwas examined by means of various additives. There is an inhibitory effect on the DNA cleavage activity by the addition of singlet oxygen quenchers like sodium azide (NaN_3). The addition of deuterated water showed enhancement of the cleavage activity, thus signifying $_1O^2$ generation plays a key role in photo cleavage of pUC 19 DNA. The hydroxyl radical scavengers like DMSO has no apparent effect on the cleavage process, thus excluding the possibility of a

type-I pathway forming hydroxyl radical (•OH). The mechanistic data suggest a photo-redox pathway for the DNA cleavage reaction of complexes via hydroxyl radical as the DNA-cleavage-active species. The type-II pathway may involve the metal-bound thiol unit generating the $_1O^2$ upon irradiation with light in a photo-redox process [38].

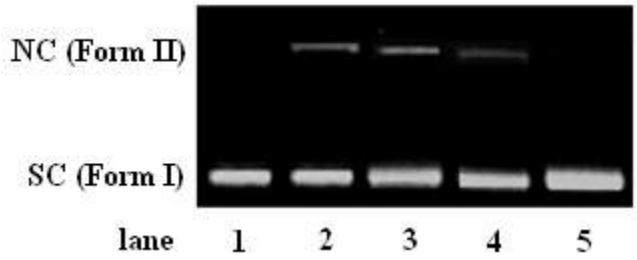

Figure 4: Gel electrophoresis diagram showing the photocleavage of SC pUC19 DNA (0.5 µg) by complex (1) (50 μM) and other additives at 365 nm for an exposure time of 1 h. lane 1, DNA control; lane 2, DNA + (1); lane 3, DNA+ (1)+ DMSO (4 µL); lane 4, DNA+ (1)+ D_2O (14 µL); lane 5, DNA+(1)+ NaN_3 (100 µM)

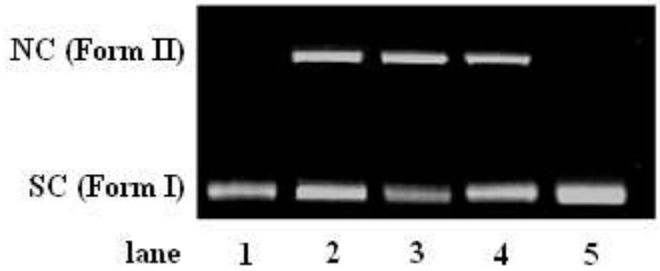

Figure 5: Gel electrophoresis diagram showing the photocleavage of SC pUC19 DNA (0.5 µg) by complex (2) (50 μM) and other additives at 365 nm for an exposure time of 1 h. lane 1, DNA control; lane 2, DNA + (2); lane 3, DNA+ (2)+ DMSO (4 µL); lane 4, DNA+ (2)+ D_2O (14 µL); lane 5, DNA+(2)+ NaN_3 (100 µM

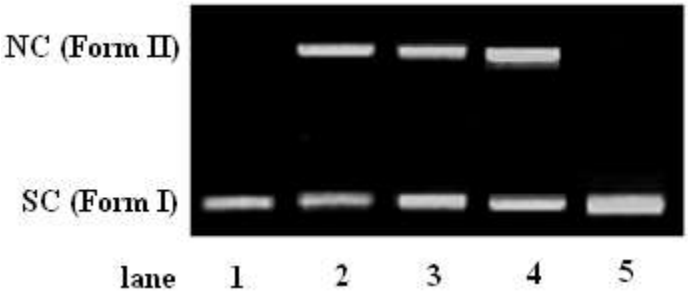

Figure 6: Gel electrophoresis diagram showing the photocleavage of SC pUC19 DNA (0.5 µg) by complex (3) (50 μM) and other additives at 365 nm for an exposure time of 1 h. lane 1, DNA control; lane 2, DNA + (3); lane 3, DNA+ (3)+ DMSO (4 µL); lane 4, DNA+ (3)+ D_2O (14 µL); lane 5, DNA+(3)+ NaN_3 (100 µM)

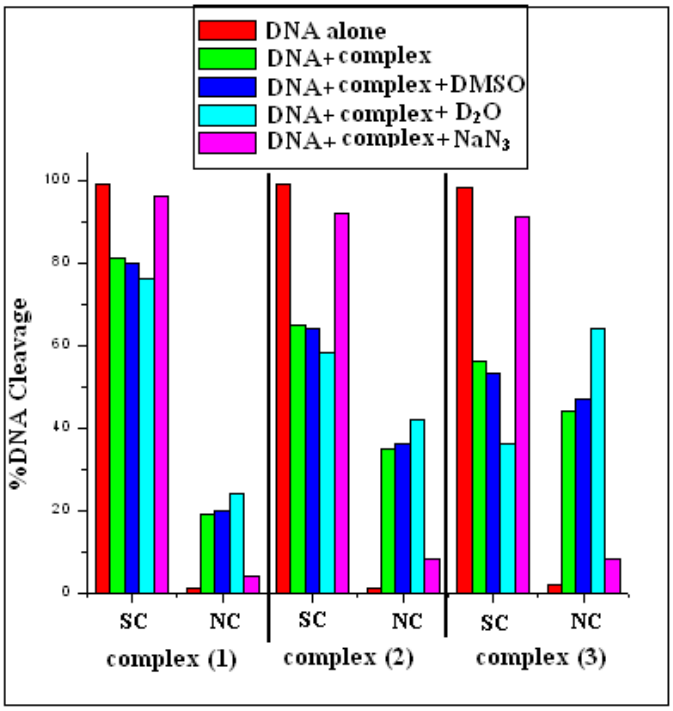

Figure 7: Cleavage of SC pUC19 DNA (50 μM) by complexes (1), (2) and (3) in the presence of various additives upon photo irradiation at 365 nm in 50 mM *Tris*-HCl / NaCl buffer (pH 7.2)

Antibacterial Photodynamic therapy (APDT)

Photodynamic therapy (PDT) is one of the greatest pledges to prevent infection progression. It involves the use of light of specific wavelength to activate a nontoxic photosensitizing agent in the presence of oxygen for eradication of target cells, and can be used for photokilling of microorganisms[39, 40]. This study evaluated *in vitro* the photodynamic effect complex (3) in combination with light source on *Escherichia coli* 25922. Suspension (2 mL) containing *Escherichia coli* at 1.5 x 10^8 CFU/ mL concentration were prepared and divided into 3 groups: Control group (no treatment), complex (3) group (inoculum and complex (3) for 5 min) and complex (3) /Light group (inoculum, complex (3) for 5 min and light for 3 min). Aliquots of undiluted and serially diluted treated and control cultures were plated on LB agar medium was performed for subsequent visual counting of CFU/mL. Counting of all CFU of E. coli strain remaining in the Control, complex (3) and complex (3) /Light groups was done to determine effectiveness of PDT. For E. coli strain, the Control group (no treatment) showed a significantly higher ($p<0.05$) bacterial growth (1.5 x 10^8 CFU/mL), while the complex (3) group presented no statistically significant ($p>0.05$) bacteria reduction, indicating that the complex (3) alone seems not to reduce bacterial viability. In the complex (3) /Light groups, however, both bacterial strains

were sensitive to the PDT protocol, presenting a significantly less expressive CFU counts ($p<0.05$) compared with the initial numbers recorded in both Control and complex (3) groups. The results of PDT on E. coli in terms of CFU counts (%) after treatment can be seen in Figure1. Statistical analysis for E. coli revealed a nonsignificant reduction (19.23%) of CFU counts between the complex (3) and Control groups. However, a significant reduction (71.64%) of CFU counts was observed for the complex (3)/Laser group compared with the Control group. Data were analyzed by one-way ANOVA and Tukey's HSD test at 5% significance level. It may be concluded that complex (3) molecule can be promising antimicrobial photosensitizer for PDT.

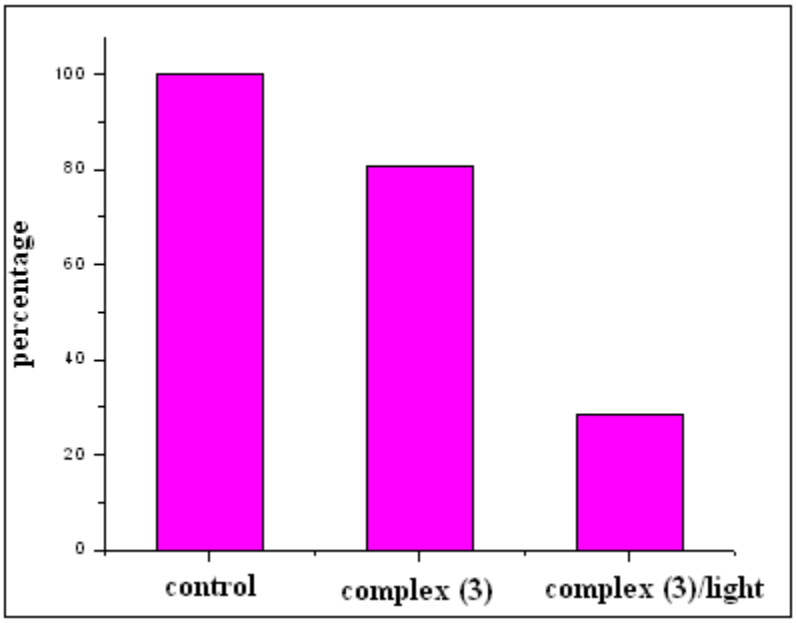

Figure 8: CFU reduction (%) in E. coli after treatments

CONCLUSION

We report here the first iron-based, low molecular- weight complexes having N, S donor of mqsH and N, N-donor heterocyclic base (B) are prepared and structurally characterized and that shows efficient DNA binding and cleavage activity. Binding study investigated by using UV-spectrophometeric, viscosity and thermal denaturation methods that shows a minor groove binding nature of the Fe(II) complexes with CT-DNA. Photoactive dpq and dppz ligands are found to play an important role in the photoinduced DNA cleavage activity under UV light. Mechanistic studies revealed direct involvement of singlet oxygen in the photo-cleavage process. These results are of importance in designing new iron-based synthetic photonucleases and making this molecule a very promising antibacterial photosensitizer. Our outcomes suggest that complex (3) should improve the efficiency of photodynamic therapy against multi resistant bacteria.

ACKNOWLEDGMENT

This work has been supported by providing Post Doctoral Fellowship for women (2009–10 & 2010–11) from the University Grants Commission, New Delhi.

REFERENCES:

1. Boerner LJK and JM Zaleski JM. Metal complex–DNA interactions: from transcription inhibition to photoactivated cleavage. Curr Opin Chem Biol 2005; 9: 135.
2. Fernandez MJ, Wilson B, Palacios M, Rodrigo MM, Grant KB and Lorente A. Copper Activated DNA Photocleavage by a Pyridine-Linked bis-Acridine Intercalator Bioconjug Chem 2007; 18: 121-129
3. Jin Y and Cowan JA. DNA cleavage by copper-ATCUN complexes. Factors influencing cleavage mechanism and linearization of dsDNA. J Am Chem Soc 2005; 127: 8408-8415.
4. Shao Y, Sheng X, Li Y, Jia Z-L, Zhang J-J, Liu F and Lu G-Y. DNA binding and cleaving activity of the new cleft molecule N,N'-bis (guanidinoethyl)-2,6-pyridinedicarboxamide in the absence or in the presence of copper (II). Bioconjug Chem 2008; 19:1840-1848.
5. Liu C-L, Wang M, Zhang T-L and Sun HZ. D**NA** hydrolysis promoted by di- and multi nuclear metal complexes. Coord Chem Rev 2004; 248:147-168.
6. Ksaprzak KS. .DNA deaminating ability and genotoxicity Chem Res Toxicol 1991; 4:604 612.
7. Ji LN, Zou XH and Liu JG. Shape- and enantioselective interaction of Ru(II)/Co(III) polypyridyl complexes with DNA. Coord Chem Rev. 2001; 216: 513–536.
8. Kane-Maguire NAP and Wheeler JK. Photoredox behavior and chiral discrimination of DNA bound M(diimine)3n+ complexes (M = Ru^{2+}, Cr^{3+}). Coord Chem Rev 2001; 211: 145–162.
9. Xiong Y and Ji L-N. Synthesis, DNA-binding and DNA-mediated luminescence quenching of Ru(II) polypyridine complexes. Coord Chem Rev 1999; 185: 711–733.
10. Mesmaeker AK, Lecomte JP and Kelly JM. Photoreactions of metal complexes with DNA, especially those involving a primary photo-electron transfer. Top Curr Chem 1996; 177: 25–76.
11. Anna JM, Sanjio SZ, Harkesh BS and Raghavan BS. Organoselenium chemistry: role of intramolecular interactions. Chem Rev 2010; 110: 4357–4416.

12. El-Bayoumy K and Sinha R. Mechanisms of mammary cancer chemoprevention byorganoselenium compounds. Mutat Res 2004; 551: 181–197.
13. Dinesh RG, Mamoru K and Hideharu I. Isoselenocyanates: A powerful tool for the synthesis of selenium-containing heterocycles. Molecules 2007; 12: 504–535.
14. Murray V and Martin RF. The sequence specificity of bleomycin-induced DNA damage in intact cells. J Biol Chem 1985; 260:10389–10391.
15. Burger RM. Cleavage of nucleic acids by bleomycin. Chem. Rev. 1998; 98:1153–1170.
16. Thomas CJ, Mc Cormick MM, Vialas C, Tao ZF, Leitheiser CJ, Rishel MJ, Wu X and Hecht SM. Alteration of the selectivity of DNA cleavage by a deglycobleomycin analogue containing a trithiazole moiety. J Am Chem Soc. 2002; 124:3875–3884.
17. Wilox DE. Binuclear metallohydrolases. Chem Rev 1996; 96: 2435–2458.
18. Yuan J, Lovejoy DB and Richardson DR. Novel di-2-pyridyl-derived iron chelators with marked and selective antitumor activity: in vitro and in vivo assessment. Blood 2004;104: 1450-1458.
19. Richardson DR, Sharpe PC, Lovejoy DB, Senaratne D, Kalinowski DS, Islam M and Bernhardt PV. Dipyridyl thiosemicarbazone chelators with potent and selective antitumor activity form iron complexes with redox activity. J Med Chem 2006; 49: 6510-6521.
20. Hoehn ST, Junker HD, Bunt RC, Turner CJ and Stubbe J. Solution Structure of Co(III)-Bleomycin-OOH Bound to a Phospho-glycolate Lesion Containing Oligonucleotide: Implications for Bleomycin-Induced Double-Strand DNA Cleavage. Biochemistry 2001; 40:5894-5905.
21. Meisel P and Kocher T Photodynamic therapy for periodontal diseases: state of the art, J. Photochem. Photobiol B: Biol 2005; 79:159–170.
22. Wainwright M. Photodynamic antimicrobial chemotherapy (PACT) J Antimicrob Chemother.1998; 42:13–28.
23. Sasmal PK, Patra AK, Nethaji M and Chakravarty AR. DNA cleavage by new oxovanadium(IV) complexes of N-salicylidene r-amino acids and phenanthroline bases in the photodynamic therapy window. Inorg Chem. 2007; 46: 1112–1121.
24. Prabahkara MC and Bhojya Naik HS.Binding and photocleavage of DNA by mixed ligand Co(III) andNi(II) complexes of thiophene[2, 3-b] quinoline and phenanthrolie/bipyridine. Biometals. 2008; 21: 675–684.
25. Ravikumar Naik TR, Bhojya Naik HS, Ramesh S, Raghavendra M and Krishnamurthy G. One-pot synthesis of 2-seleno-4-methylquinoline. Molbank 2007; M543.

26. Nandeshwarappa BP, Arun Kumar DB, Bhojya Naik HS and Mahadevan KT. An efficient microwave-assisted synthesis of thieno[2,3- *b*]quinolines under solvent-free conditions J Sulphur Chem. 2005; 26: 373.
27. Yamada M, Tanaka Y, Yoshimoto Y, Kuroda S and Shimao I. Synthesis and Properties of Diamino-Substituted Dipyrido [3,2-*a*: 2′,3′-*c*]phenazine Bull. Chem Soc Jpn. 1992; 65:1006-1011.
28. Collins JG, Sleeman AD, Janice RAW, Greguric I and Hambley TW. A ^{1}H NMR Study of the Binding of Ruthenium(II) Polypyridyl Complexes Inorg Chem 1998; 37: 3133-3141.
29. Dupureur CM and Barton JK. Structural Studies of L- and D-[Ru(phen)2dppz]2+ Bound to d(GTCGAC)$_2$: Characterization of Enantioselective Intercalation Inorg Chem 1997; 36: 33-43.
30. Sudhamani CN, Bhojya Naik HS and Girija D. Synthesis and Reactivity in Inorganic, Metal-Organic, and Nano-Metal Chemistry, 2012; 42:518–524,
31. Lamour E, Routier S, Bernier JL, Bailly C and Vezin HJ. Oxidation of CuII to CuIII free radical production and DNA cleavage by hydroxy-salen-copper complexes: isomeric effects studied by ESR and electrochemistry. J Am Chem Soc. 1999; 121:862–863.
32. Nair R B, Teng E S, Kirkland SL and Murphy CJ, Synthesis and DNA-Binding Properties of [Ru(NH(3))(4)dppz](2+). Inorg Chem. 1998; 37: 139-141.
33. Sathyanarayana S: Dabrowiak JC and Chaires JB. Tris(phenanthroline) ruthenium(II) enantiomer interactions with DNA: mode and specificity of binding. J Biochem. 1993; 32: 2573–2584.
34. Xiong Y, He XF, Zou XH, Wu JZ, Chen XM, Ji LN, Li R.H, Zhou JY and Yu KB. Interaction of polypyridyl ruthenium(II) complexes containing non-planar ligands with DNA. J Chem Soc Dalton Trans. 1999; 19–24.
35. Lincoln P and Nord´en B. DNA binding geometries of ruthenium(II) complexes with 1,10-phenanthroline and 2,2_-bipyridine ligands studied with linear dichroism spectroscopy. Borderline cases of intercalation. J Phys Chem B 1998; 102: 9583–9594.
36. Sethuraman M and Mallayan P. Spectroscopic and voltammetric studies on copper complexes of 2,9- dimethyl-1,10-phenanthrolines bound to calf thymus DNA. Inorg Chem 1998; 37:693–700.
37. Fu PKL, Bradley PM and Turro C. Stabilization of duplex DNA structure and suppression of transcription in vitro by bis(quinone diimine) complexes of rhodium(III)

and ruthenium(II) Inorg Chem. 2003; 42 878-884.

38. Mithun Roy, Biswarup Pathak, Ashis K. Patra, Eluvathingal D. Jemmis, Munirathinam Nethaji, and Akhil R. Chakravarty. Inorg Chem. New insights into the visible-light-induced DNA cleavage activity of dipyridoquinoxaline complexes of bivalent 3d-metal ions. 2007; 46: 11123-11132.
39. Xavier Ragas, David Sanchez-G. Ruben Ruiz Gonzalez, Tianhong D, Montserrat Agut, Michael R, Hamblin and Santi Nonell, Cationic Porphycenes as Potential Photosensitizers for Antimicrobial Photodynamic Therapy. J Med Chem 2010; 53: 7796–7803.
40. Annie Shrestha and Anil Kishen. Polycationic Chitosan-Conjugated Photosensitizer for Antibacterial Photodynamic Therapy. Photochemistry and Photobiology, 2012; 88: 577–583.